1 2	Robust yet Diverse Tropical Responses to Antarctic Meltwater Across Models
3	Xiyue Zhang <sup>1</sup> , Ariaan Purich <sup>2</sup> , Clara Deser <sup>3</sup> , and Andrew Pauling <sup>4</sup>
4	<sup>1</sup> Department of Physics, University of Nevada, Reno, USA.
5 6 7	<sup>2</sup> School of Earth, Atmosphere and Environment, and ARC Special Research Initiative for Securing Antarctica's Environmental Future, Monash University, Clayton, Kulin Nations, VIC, Australia.
8	<sup>3</sup> National Center for Atmospheric Research, Boulder, CO, USA.
9	<sup>4</sup> Department of Physics, University of Otago, Dunedin, New Zealand.
10	
11 12	Corresponding author: Xiyue Zhang (xiyuez@unr.edu)
13	Key Points:
14 15	<ul> <li>Coupled models robustly simulate tropical cooling and a northward ITCZ shift in response to Antarctic meltwater input but vary in magnitude</li> </ul>
16 17	<ul> <li>Models with stronger subtropical low cloud feedbacks tend to show a larger tropical-to- Southern Ocean cooling ratio</li> </ul>
18 19	<ul> <li>Surface energy budget analysis suggests model-dependent and basin-dependent teleconnection pathways and timescales</li> </ul>

#### **Abstract**

Continued melting of Antarctic ice sheets and shelves introduces freshwater into the Southern Ocean (SO), enhancing stratification and surface cooling. This cooling influences tropical climate through coupled atmosphere—ocean pathways, though the magnitude of the response varies across models. Using a coordinated suite of coupled model experiments with idealized Antarctic meltwater forcing, we assess the remote impacts of SO surface cooling. All seven models simulate equatorial surface cooling and a northward displacement of the Intertropical Convergence Zone, but the equatorial Pacific zonal sea surface temperature gradient and Atlantic meridional dipole exhibit substantial intermodel spread. When normalized by each model's SO cooling amplitude, these tropical metrics are positively correlated with shortwave cloud feedback strength. The timescale of tropical cooling and the relative roles of wind-driven latent heat and shortwave fluxes differ across models and basins, underscoring the need for further investigation of SO—tropics teleconnections.

### **Plain Language Summary**

Melting of Antarctic ice sheets and ice shelves adds freshwater to the Southern Ocean, causing the surface ocean to become more stratified and cooler. Earlier studies suggest that this Southern Ocean cooling can influence tropical climates through changes in ocean and atmospheric circulation. However, current climate models do not include interactive ice sheets and therefore miss this meltwater effect. In this study, we analyze results from seven climate models with imposed Antarctic meltwater to test how consistently they simulate these remote impacts. All models show cooling that extends into the tropics, but they differ in how strong this cooling is and where it occurs. By examining the surface energy budget, we find that the processes linking the Southern Ocean to the tropics vary among models and between the Pacific and Atlantic Oceans. These differences highlight the need for better understanding of how Antarctic meltwater influences global climate.

#### 1 Introduction

It is well established that extratropical forcing can impact tropical climate via coupled atmosphere-ocean processes (Liu & Alexander, 2007; Seo et al., 2014; Kang et al., 2019). Observed concurrent cooling in the tropical eastern Pacific and Southern Ocean (SO) over recent decades (Wills et al., 2022) has spurred renewed interest in this teleconnection pathway (Hwang et al., 2017; Zhang et al., 2021; Kim et al., 2022; Kang et al., 2023; Dong, Armour, et al., 2022; Zhang & Deser, 2024). The eastern Pacific cooling has enhanced the zonal sea surface temperature (SST) gradient across the basin, contributing to what is often referred to as the "pattern effect"—a phenomenon linking spatial variations in warming magnitude to climate sensitivity (Stevens et al., 2016; Rugenstein et al., 2023). Recent studies suggest that teleconnections originating from the Southern Ocean can influence observed tropical Pacific SST trends (Kang et al., 2023; Zhang & Deser, 2024; Dong et al., 2025), underscoring the SO's role in modulating global climate feedbacks. Understanding the pattern effect and improving confidence in future climate projections thus requires improved understanding of the drivers behind SO SST trends and the mechanisms by which high-latitude changes influence the tropics.

Previous studies based on various experimental protocols have shown that Southern Ocean cooling induces surface cooling over the tropical southeast Pacific and South Atlantic, as well as a northward shift of the inter-tropical convergence zone (ITCZ) (Kang et al., 2019; Kim et al., 2022). This Southern Ocean teleconnection pathway was hypothesized to initiate from climatological northward advection of the Southern Ocean SST anomalies into the subtropical southeast Pacific. There, the shortwave low-cloud feedback, wind-evaporation-surface temperature feedback, and coastal upwelling amplify the local surface temperature anomalies. The anomalies may either remain in the subtropical regions or penetrate into the equatorial Pacific where the Bjerknes feedback further intensifies the cooling (Kim et al., 2022). Questions remain whether this teleconnection pathyway operates across different coupled climate models, and if the same pathway exists in the tropical South Atlantic.

Several factors may contribute to the recent cooling of the SO, although models generally fail to reproduce the observed magnitude (Wills et al. 2022). The SO mean-state circulation characterized by upwelling of deep, relatively unaltered waters—limits surface warming under anthropogenic climate change compared to other regions (Armour et al., 2016). In addition, several mechanisms have been proposed to explain the observed SO cooling during the satellite era, which coincided with an increase in Antarctic sea ice extent until around 2014 (e.g., Fan et al., 2014; Purich, Cai, et al., 2016; Purich, England, et al., 2016; Dong et al., 2025). Accelerating Antarctic meltwater input has emerged as a potential driver of SO surface cooling (Rye et al., 2020; Dong, Pauling, et al., 2022; Roach et al., 2023; Kaufman et al., 2025). Freshwater influx enhances stratification, suppressing vertical mixing and entrainment of warmer subsurface waters, thereby promoting surface cooling (e.g., de Lavergne et al., 2014; Morrison et al., 2015; Purich et al., 2018). Importantly, coupled climate models participating in CMIP6 do not incorporate dynamic ice sheets and shelves (Eyring et al., 2016; Swart et al., 2023) and thus omit the meltwater-induced cooling effect. This omission leads to uncertainty in climate projections (Bronselaer et al., 2018; Fyke et al., 2018; Golledge et al., 2019; Sadai et al., 2020) and may contribute to the models' inability to reproduce observed SO SST trends.

The climatic influence of Antarctic meltwater has been widely studied (e.g., see Table 1 in Swart et al. (2023)), but differences in model configurations and experimental designs have hindered cross-study comparisons. To address this, the Southern Ocean Freshwater Input from Antarctica (SOFIA) Initiative introduced a standardized meltwater forcing protocol, enabling consistent assessment of meltwater impacts across an ensemble of coupled models (Swart et al., 2023). In this study, we leverage the SOFIA ensemble to investigate the pathways through which SO meltwater-induced cooling affects the tropical Pacific and Atlantic Oceans.

Here, we find that the SOFIA multimodel mean reveals cooling in both the eastern tropical Pacific and equatorial Atlantic, in response to Antarctic meltwater additions. Across the ensemble, variations in the magnitude of SO cooling are linked to changes in the Pacific zonal SST gradient and the Atlantic Meridional Mode. These responses are modulated by the strength of shortwave cloud feedback across models, highlighting this feedback as a key process governing high-latitude to tropical teleconnections.

#### 2 Data and Methods

A detailed description of the SOFIA protocol and simulations can be found in Swart et al. (2023). Briefly, we make use of output from the idealized *antwater* experiment, which is branched off the CMIP6 *piControl* simulation. A freshwater flux anomaly of 0.1 Sv is applied at the surface in Antarctic-adjacent ocean grid cells. This freshwater flux is about 10 times the estimated historical freshwater flux anomaly by 2020, and about a half of the projected basal

melt input by 2010 in the high-end emission scenario (ssp585, Fig. A1 from Swart et al. (2023)). All other forcings are the same as in *piControl*. The antwater simulations are 100 years long. We define the response to Antarctic meltwater input as the annual mean anomalies of antwater simulations, which are calculated as the difference between the *antwater* average from Year 51 to 100 and the *piControl* average of 100 years.

We focus on seven models: ACCESS-ESM1-5 (Ziehn et al., 2020), CanESM5 (Swart et al., 2019), CESM2 (Danabasoglu et al., 2020), GFDL-CM4 (Held et al., 2019), GFDL-ESM4 (Dunne et al., 2020), GISS-E2-1-G (Kelley et al., 2020), HadGEM3-GC3.1-LL (Kuhlbrodt et al., 2018), and based on data availability at the time of this study. Most models only have one ensemble member, but in the three models (CanESM5, ACCESS-ESM1-5, and CESM2) with multiple members, the first ensemble member from every model is used for the model intercomparison (Figure 1–3). The model outputs were regridded onto a common 1° horizontal grid. For the surface energy budget, we analyze outputs from CESM2 and ACCESS-ESM1-5, as the needed variables are not available from other models. These two models each have a small ensemble branched from different years of the *piControl* simulations: three members for CESM2 and five members for ACCESS-ESM1-5. We use the ensemble mean (CESM-EM and ACCESS-EM) for the surface energy budget analysis to reduce the noise from internal variability on the tropical response (Figure 4).

We perform an energy budget analysis of the mixed layer ocean to provide insight into the physical mechanisms of the SO to tropical teleconnection, following Xie et al. (2010) and Kang et al. (2023). The surface energy balance is given by  $\rho C_p H \frac{\partial T}{\partial t} = SW + LW - LH - SH + O$ . The left-hand side represents heat storage:  $\rho$  is ocean density,  $C_p$  is the specific heat of water, and H is the mixed-layer depth, and T is the mixed-layer temperature (taken as the surface temperature). The right-hand side includes the shortwave flux (SW), longwave flux (LW), latent heat flux (LH), sensible heat flux (SH), and ocean dynamics (O). At quasi-equilibrium, the heat storage anomaly is close to zero, so that the ocean dynamics anomaly is calculated as a residual. In a transient state, the heat storage is not negligible but small compared to other terms (Figure 4). Therefore, the ocean dynamics term largely represents the effect of horizontal advection and upwelling/downwelling.

By linearizing the bulk aerodynamic formula for latent heat flux, we can rewrite and diagnose the mixed-layer temperature anomaly  $\Delta T$  as:  $\Delta T = \frac{1}{\alpha L H} (\Delta SW + \Delta LW - \Delta SH + \Delta O - \Delta LH_{others})$ , where  $\Delta$  denotes the response (e.g., antwater minus piControl), overbar denotes the piControl mean,  $\alpha = \frac{L_v}{R_v T^2} \approx 0.06 \text{ K}^{-1}$  where  $L_v$  is the latent heat of vaporization and  $R_v$  is the gas constant of moist air. The term  $\Delta LH_{others} = \Delta LH - \alpha \overline{LH}\Delta T$  represents the combined effects of wind speed, relative humidity, and air-sea temperature difference on latent heat flux. Previous studies have shown that wind speed changes often dominate the latent heat flux in the tropical and subtropical oceans (Zhang et al., 2021; Kang et al., 2023). We diagnose the surface temperature anomalies from all terms on the right-hand side for each year.

#### 3 Results

The multi-model mean (MMM) near-surface air temperature (TAS) shows robust SO cooling in response to Antarctic meltwater forcing (Figure 1a) as expected, given that the meltwater forcing is added to the surface around the Antarctic coast (Swart et al., 2023). All

seven models analyzed here show a surface cooling response throughout the Southern Hemisphere, with the cooling gradually weakening towards the equator. The South Pacific shows a prominent zonal asymmetry in its TAS response, where the cooling is strongest in the southeastern portion of the basin and weakest around the Maritime Continent. In the North Pacific, weak warming is evident in the west with cooling in the east, a pattern reminiscent of the negative phase of Pacific Decadal Variability (Mantua et al., 1997), although this response is only present in six models (stippling on Figure 1a, also see Figure S1). In the Atlantic, cooling gradually weakens northward from the Southern Ocean up to around 40°N. The region of positive TAS anomaly aligns with the location of the North Atlantic "warming hole", a region of reduced warming identified in coupled climate models in response to greenhouse gas forcing. The Arctic shows amplified cooling compared to lower latitudes, a robust response across all models.

 While models show agreement on the sign of the TAS response to meltwater input, there is large spread in the magnitude of their responses. In the zonal-mean, the largest spread in TAS response is found over the SO (Figure 1b). While all models display the strongest cooling at around 65°S, the magnitude varies between -3 K to -1.4 K, which is likely due to different model response in Southern Ocean deep convection (Chen et al., 2023). Interestingly, models with the strongest SO cooling, namely CanESM5 and GFDL-ESM4, do not have the strongest tropical cooling. For example, CESM2 simulates the strongest equatorial cooling of all the models (-0.38 K), yet its SO cooling the second weakest (-1.5 K). In the Arctic, the TAS cooling is slightly amplified, ranging from -0.8 to -0.2 K across models. This model spread is indicative of a range of SO teleconnection strength across models.

Accompanying the TAS response, the precipitation response shows unanimous drying over the SO that extends into the Southern Hemisphere subtropics (Figure 1c). The dipole precipitation response in the tropical Pacific is consistent with a northward shift of the ITCZ. In the Atlantic, we also find a northward ITCZ shift with a positive precipitation anomaly extending across the Sahel. Models agree on the sign of these tropical precipitation anomalies (stippling on Figure 1c), except for the negative anomaly in the far western tropical Pacific. The northward ITCZ shift is consistent with zonal-mean energetic arguments whereby precipitation shifts away from the cooler Southern Hemisphere (Kang, 2020).

The zonal-mean precipitation response shows the largest inter-model spread in the tropics (Figure 1d), perhaps not surprisingly, given the large variation of climatological precipitation in the tropics across models (not shown). All models show the precipitation anomaly maximum in the Northern Hemisphere, while the precipitation minimum is in either hemisphere depending on the model. The magnitudes of the zonal-mean precipitation extremes also vary greatly across

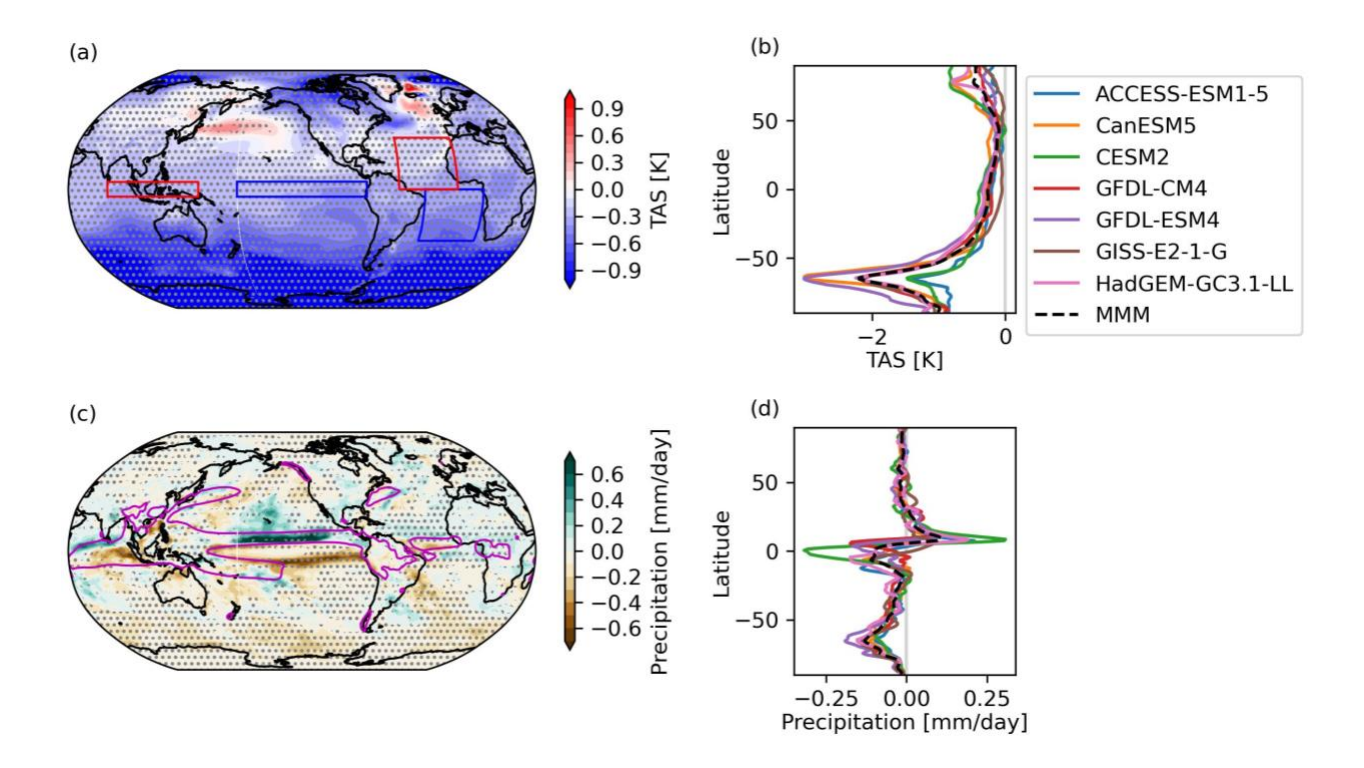


**Figure 1**: Response of near-surface air temperature (TAS) and precipitation (PR) to *antwater* forcing. (a) Multi-model mean (MMM) TAS response. (b) Zonal-mean TAS response from individual models and MMM. (c) MMM PR response. Magenta contours indicate the MMM *piControl* precipitation of 5 mm/day. (d) Zonal-mean PR response from individual models and MMM. Stippling on the maps indicates agreement in the sign of the response among at least six out of seven models. Red and blue boxes in panel (a) are regions used to calculate metrics in Figure 3.

models: CESM2 shows the largest tropical precipitation anomalies of +/- 0.3 mm/day, more than twice the magnitude of the MMM anomalies.

Next, we focus on the zonal asymmetry of the equatorial Pacific (5°S–5°N) TAS *antwater* response. The tropical Pacific zonal temperature gradient is an indicator of the Walker circulation strength (Watanabe et al., 2024). Previous studies have pointed out that southern extratropical forcing tends to influence the Walker circulation via changing the tropical Pacific zonal temperature gradient, as surface temperature anomalies tend to preferentially propagate along the eastern ocean basin (Kang et al., 2019). The SOFIA MMM TAS response shows a modest strengthening of the equatorial Pacific zonal temperature gradient, with maximum cooling (-0.31 K) in the east and minimum cooling (-0.17 K) near the Maritime Continent (Figures 1a and 2a). While six out of seven models agree with this general strengthening pattern (stippling on Figure 1a), the magnitude and longitude of maximum cooling varies greatly. For example, the two end members, GISS-E2-1-G and CESM2, have opposing TAS anomalies of 0.13 K and -0.57 K in the central and eastern Pacific.

In the Atlantic, we focus on the tropical SST dipole across the equator, which is a major driver of North Atlantic hurricane and Sahel rainfall variabilities (Chang et al., 1997; He et al., 2023). All models consistently show a strengthening of the tropical Atlantic meridional

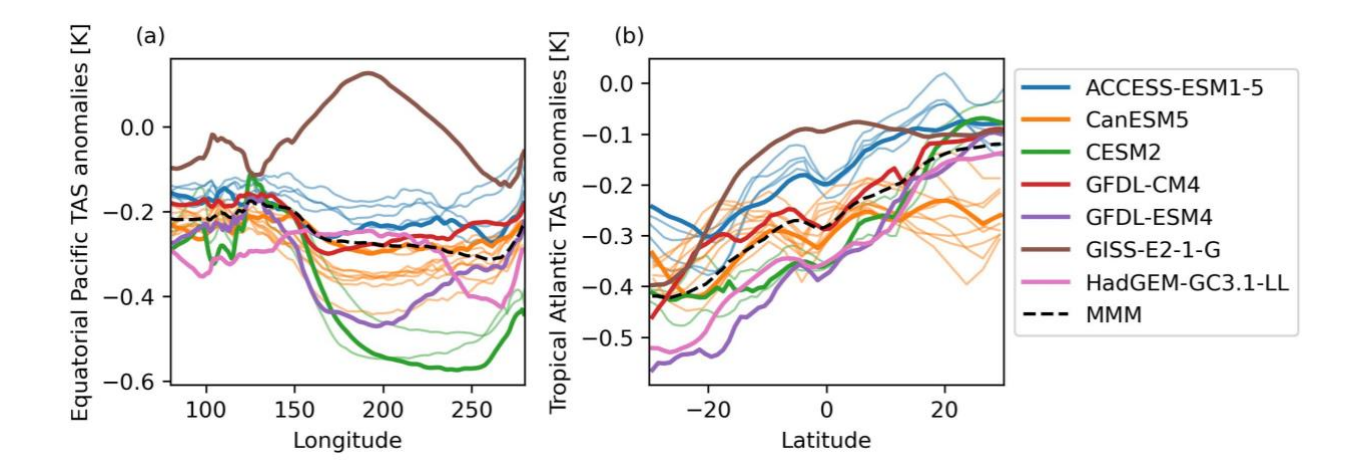


**Figure 2**: Tropical Pacific and Atlantic TAS responses. (a) Equatorial Pacific (5°S–5°N) average as a function of longitude. (b) Tropical Atlantic (60°W–0°) average as a function of latitude. Light thin lines show additional ensemble members from CanESM5, ACCESS-ESM1-5, and CESM2.

temperature gradient, with greater cooling near 30°S (-0.42 K) compared to 30°N (-0.12 K) in the MMM (Figure 2b). However, there is a substantial (0.2 K) inter-model spread in the magnitude of the tropical Atlantic gradient response. A notable outlier is GISS-E2-1-G, which shows strengthened meridional TAS gradient confined to the Southern Hemisphere.

To account for the spread in the SO cooling response to the standardized meltwater forcing across the SOFIA ensemble, we normalize both tropical metrics by the SO TAS anomalies (75°S–50°S) to calculate a response ratio (see Figure S2 for anomalies without normalization). The inter-model spread in both the tropical Pacific zonal temperature gradient and the tropical Atlantic meridional dipole can be largely explained by the strength of the subtropical shortwave cloud feedback (Figure 3). Here the feedback is defined as the regression of shortwave cloud radiative effect anomalies on local surface temperature anomalies, calculated for the west coast of South America (Table S1 in Kim et al., 2022). CESM2 shows the strongest shortwave cloud feedback, and has the strongest normalized response in both the Pacific and Atlantic. On the other hand, GISS-E2-1-G shows the weakest shortwave cloud feedback and has the weakest normalized response, which is of the opposite sign in the tropical Pacific. The shortwave cloud feedback strength explains 89% of the intermodel spread of Pacific zonal temperature gradient and 57% of the intermodel spread in the tropical Atlantic meridional dipole. All models except for CESM2 underestimate the shortwave cloud feedback strength compared to observationally derived values of around 7.4 W/m² (Kim et al., 2022).

We also find a sizable ensemble spread in the tropical response ratios in the three models with multiple ensemble members. In the tropical Pacific, the zonal temperature gradient response ratio shows a spread of approximately 0.1 across individual members (Figure 3a), indicating that internal variability can influence the magnitude of the SO teleconnection even when the forcing is strong. In the Atlantic, CanESM5 shows an ensemble spread of 0.18 in the tropical Atlantic dipole response ratio, which is larger than that of CESM2 and ACCESS-ESM1-5 (Figure 3b).

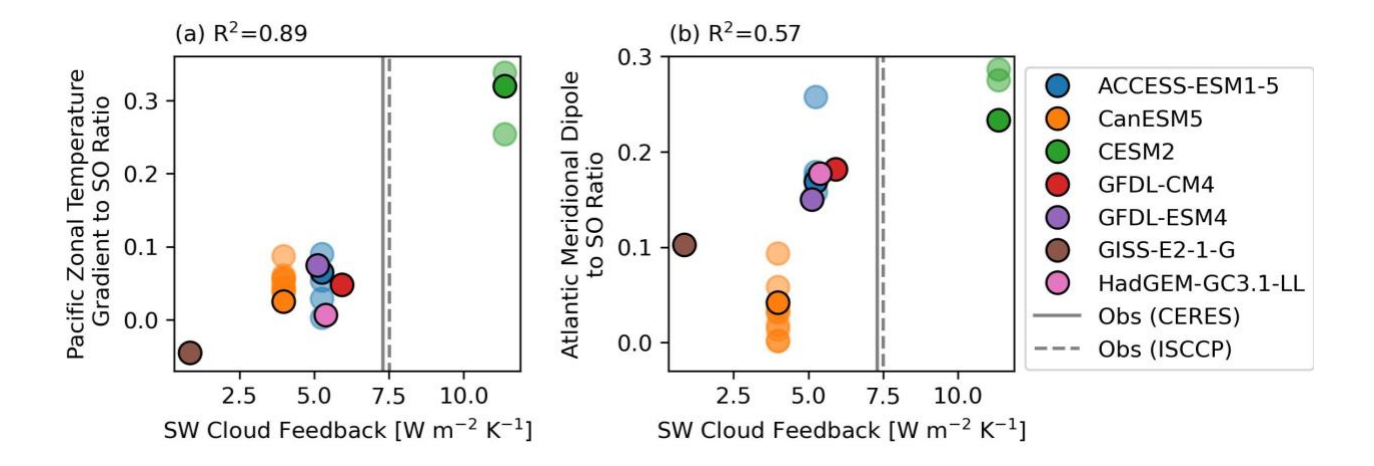


**Figure 3**: Response ratio of (a) Equatorial Pacific zonal temperature gradient (Figure 1a red box minus blue box in the Pacific) and (b) Atlantic meridional dipole (Figure 1a red box minus blue box in Atlantic) to Southern Ocean temperature, as a function of shortwave cloud feedback strength in the subtropical southeast Pacific. Individual ensemble members from CanESM5, ACCESS-ESM1-5 and CESM2 are shown in lighter shaded circles without black outlines. Correlations (in panel titles) are calculated for only the first ensemble member of each model.

This suggests that internal variability may be as important as model uncertainty in the quasiequilibrium response to extratropical forcing.

To better understand the inter-model spread in the tropical temperature response to Antarctic meltwater forcing, we analyze the surface heat budget of the ocean mixed layer response in the CESM2 and ACCESS-ESM1-5 ensemble means (there is substantial variation in the budget evolution across individual members, see Figure S3 and S4). We focus on the equatorial Pacific and tropical South Atlantic regions (black boxes in Figure 4a and 4b), as they directly contribute to the equatorial Pacific zonal surface temperature gradient and the tropical Atlantic dipole. We further divide the equatorial Pacific region into a central box (180°–130°W) and an eastern box (130°W–80°W), as the dynamics differ in the two regions. While most surface energy budget analyses focus on the equilibrium response (e.g., Hwang et al., 2017), here we examine the temporal evolution of individual budget terms (Figure 4c–f).

CESM2 shows a strong tropical Pacific cooling of about 0.5 K at equilibrium (Figure 4c and 4e). The latent heat term contributes to cooling in both the central and eastern Pacific. However, the shortwave term cools the eastern Pacific but warms the central Pacific, while the ocean dynamics term warms the eastern Pacific but cools the central Pacific. Interestingly, both regions shows warming in the initial years. The eastern Pacific shortwave and latent heat terms switch signs between Years 1 and 2, which leads to cooling in the region that persists for the rest of the simulation. This demonstrates the importance of the positive shortwave cloud feedback and wind-evaporation-SST feedback in amplifying and prolonging the local cooling.

The tropical Pacific cooling in ACCESS-ESM1-5 at equilibrium is weaker than that in CESM2, but the budget decomposition is similar for the easetern Pacific (Figure 4d and 4f). In the central Pacific, cooling is dominated by the ocean dynamics term, while the shortwave term makes a secondary contribution. However, the initial eastsern Pacific response shows warming that sustained for nearly a decade, much longer than the initial warming in CESM2. It takes 15

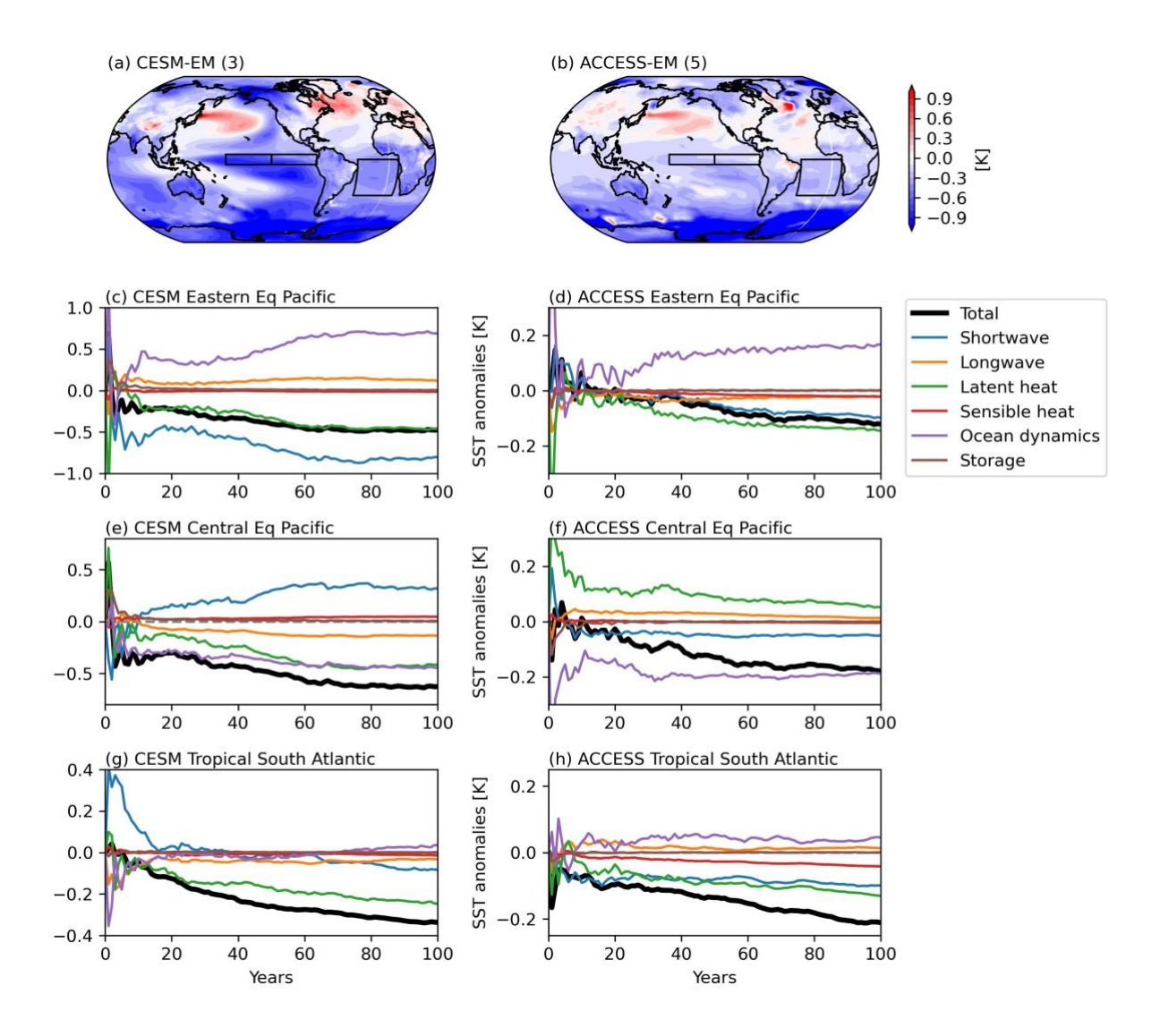


**Figure 4**: Ensemble mean surface temperature anomalies from (a) CESM2 (three members), and (b) ACCESS-ESM1-5 (five members). Regional average (outlined by black boxes) timeseries of the terms in the surface energy budget for the eastern equatorial Pacific (130°W–80°W, 5°S–5°N), central equatorial Pacific (180°–130°W, 5°S–5°N), and tropical south Atlantic (35°W–10°E, 35°S–0°) are shown in (c)–(h). The ocean dynamics term is calculated as the residual of the surface energy budget.

years for the net temperature anomaly to become consistently negative. The timescale for ACCESS-ESM1-5 to reach a negative eastern Pacific surface temperature anomaly is much longer than for CESM2.

In the tropical South Atlantic, both models show cooling dominated by the latent heat and shortwave terms at equilibrium. However, they have drastically different initial responses. CESM2 shows a gradual cooling driven by the ocean dynamics and longwave terms in the first 10 years (Figure 4g). During this time, the shortwave term remains positive, balancing the surface cooling. ACCESS-EMS1-5, on the other hand, shows a strong cooling in the first year, dominated by the shortwave and latent heat terms (Figure 4h). The contrasting initial heat budget

response in the two basins highlights potentially different pathways of regional SO teleconnections.

The two models analyzed here show different heat budget decompositions and timescales of eastern equatorial Pacific surface temperature response. The ocean dynamics term is positive for the initial years, while the latent heat term is a main contributor to cooling in both models. The shortwave term contributes to a more sizable cooling in CESM2 than in ACCESS-ESM1-5. CESM2 shows cooling by Year 3 which is consistent with Kim et al. (2022), while ACCESS-ESM1-5 did not show a sustained cooling until Year 15. However, the shortwave term leads the net cooling in CESM2 by 1 year, suggesting the shortwave cloud feedback's active role. This is not found in ACCESS-ESM1-5, as the shortwave term remains small and positive after Year 2. In the tropical Atlantic, both models reach a consistent cooling state more quickly compared to the equatorial Pacific, especially ACCESS-ESM1-5; this cooling is primarily driven by the shortwave term. While the shortwave term is a big contributor to eastern equatorial Pacific cooling in CESM2, it warms the tropical Atlantic until Year 15.

## 4 Summary and Discussion

In this study, we make use of an ensemble of seven coupled climate models running the SOFIA idealized Antarctic meltwater experiment to investigate the remote impact of SO surface cooling. In quasi-equilibrium, all models show widespread cooling extending far beyond the SO, reaching across most ocean basins and over land, except in the western/central North Pacific and subpolar North Atlantic. A northward shift of the ITCZ in the Pacific and Atlantic is found in all models. However, models disagree on the magnitude of the temperature and precipitation responses to consistent meltwater forcing. The responses of the equatorial Pacific zonal temperature gradient and the Atlantic meridional dipole both show large inter-model spread. When normalized to each model's SO response, these two tropical metrics are positively correlated with the shortwave cloud feedback strength. In the low cloud regions, a cooler surface temperature often leads to stronger boundary layer inversion strength and greater low cloud cover (Klein et al., 2017). This reduces the absorbed shortwave radiation at the surface, which further enhances cooling. This local positive feedback allows SO cooling to be enhanced along the west coast of South America, and cooler surface temperatures can further propagate into the lower latitudes via the wind-evaporation-SST feedback (Kim et al., 2022). The surface energy budget sheds light on the distinct evolution of the tropical surface temperature response in the Pacific and Atlantic in two of the models.

Most SO teleconnection studies focus on the Pacific response, as the observed eastern equatorial Pacific cooling remains a challenge for climate models to simulate. Our results confirm earlier studies that the tropical response to SO cooling depends on two key processes: the shortwave cloud feedback and the wind-evaporation-SST feedback (Figure 4c and 4d). Models with stronger subtropical shortwave cloud feedback tend to show a stronger tropical response (Figure 3a). We demonstrate in two models with different shortwave feedback strengths that the timescale of response is also sensitive to the cloud feedback. The stronger-than-observed shortwave cloud feedback in CESM2 allows the eastern equatorial Pacific to quickly cool within the first three years, while the weaker-than-observed shortwave cloud feedback in ACCESS-ESM1-5 was not a main driver of the eastern equatorial Pacific cooling. Indeed, it takes nearly 15 years for ACCESS-ESM1-5 to reach a sustained cooling state, largely from the wind-driven evaporation and longwave feedbacks. The leading hypothesis of SO teleconnection in the Pacific

from Kim et al. (2022) is based on results from a single climate model. Our results show that the proposed mechanism may be highly model dependent, and highlight the value of assessing the teleconnection across multiple models with a common experimental design.

Our study also highlights a potentially different teleconnection pathway in the tropical Atlantic. The tropical Atlantic response to Southern Ocean cooling tends to display a cross-equatorial dipole pattern, with potential implications for Sahel rainfall and hurricane impacts. The stratocumulus cloud deck off the west coast of Africa provides a strong local shortwave cloud feedback, similar to the southeast Pacific (Kim et al., 2022). In CESM2, the shortwave feedback makes a smaller contribution to the tropical south Atlantic cooling than to the eastern Pacific cooling at quasi-equilibrium. In fact, its initial contribution in the tropical Atlantic opposes the cooling. Future work will explore the basin-specific teleconnection pathways in various climate models in more detail.

## Acknowledgments

AP was supported by the Australian Research Council Special Research Initiative for Securing Antarctica's Environmental Future (SR200100005). CD was supported by the National Center for Atmospheric Research (NCAR), which is sponsored by the National Science Foundation under Cooperative Agreement 1852977. Significant effort has been invested by the SOFIA team to design the experiments, the modelers to run the experiments, and by the project members to house the data in an open common archive. Further details are available at https://sofiamip.github.io/ and described in Swart et al. (2023). We specifically thank Torge Martin and Neil Swart for coordinating SOFIA, and those who contributed the antwater experiments used in this study: Qian Li (GISS-E2-1-G), Neil Swart (CanESM5), Rebecca Beadling and Stephen Griffies (GFDL-CM4 and GFDL-ESM4), Ariaan Purich (ACCESS-ESM1-5), Max Thomas (HadGEM3-GC31-LL) and Andrew Pauling (CESM2) for making their data publicly available, and Neil Swart for for processing and documenting antwater output across the model ensemble.

## **Open Research**

The authors acknowledge the use of various data sets that significantly contributed to this research. The data of the freshwater experiments are available in Swart et al. (2023), the CMIP6 *piControl* experiments Eyring et al. (2016). Surface energy budget data for ACCESS-ESM1-5 and CESM2 are available at https://doi.org/10.5281/zenodo.17460002.

#### **Conflict of Interest Disclosure**

The authors declare there are no conflicts of interest for this manuscript.

# References

- Bronselaer, B., Winton, M., Griffies, S. M., Hurlin, W. J., Rodgers, K. B., Sergienko, O. V.,
- Stouffer, R. J., & Russell, J. L. (2018). Change in future climate due to Antarctic
- meltwater. *Nature*, 564(7734), 53–58. https://doi.org/10.1038/s41586-018-0712-z

340	Chang, P., Ji, L., & Li, H. (1997). A decadal climate variation in the tropical Atlantic Ocean
341	from thermodynamic air-sea interactions. <i>Nature</i> , 385(6616), 516–518.
342	https://doi.org/10.1038/385516a0
343	Chen, JJ., Swart, N. C., Beadling, R., Cheng, X., Hattermann, T., Jüling, A., Li, Q., Marshall,
344	J., Martin, T., Muilwijk, M., Pauling, A. G., Purich, A., Smith, I. J., & Thomas, M.
345	(2023). Reduced Deep Convection and Bottom Water Formation Due To Antarctic
346	Meltwater in a Multi-Model Ensemble. Geophysical Research Letters, 50(24),
347	e2023GL106492. https://doi.org/10.1029/2023GL106492
348	Danabasoglu, G., Lamarque, JF., Bacmeister, J., Bailey, D. A., DuVivier, A. K., Edwards, J.,
349	Emmons, L. K., Fasullo, J., Garcia, R., Gettelman, A., Hannay, C., Holland, M. M.,
350	Large, W. G., Lauritzen, P. H., Lawrence, D. M., Lenaerts, J. T. M., Lindsay, K.,
351	Lipscomb, W. H., Mills, M. J., Strand, W. G. (2020). The Community Earth System
352	Model Version 2 (CESM2). Journal of Advances in Modeling Earth Systems, 12(2),
353	e2019MS001916. https://doi.org/10.1029/2019MS001916
354	de Lavergne, C., Palter, J. B., Galbraith, E. D., Bernardello, R., & Marinov, I. (2014). Cessation
355	of deep convection in the open Southern Ocean under anthropogenic climate change.
356	Nature Climate Change, 4(4), Article 4. https://doi.org/10.1038/nclimate2132
357	Dong, Y., Armour, K. C., Battisti, D. S., & Blanchard-Wrigglesworth, E. (2022). Two-way
358	teleconnections between the Southern Ocean and the tropical Pacific via a dynamic
359	feedback. Journal of Climate, 1(aop), 1–37. https://doi.org/10.1175/JCLI-D-22-0080.1
360	Dong, Y., Pauling, A. G., Sadai, S., & Armour, K. C. (2022). Antarctic Ice-Sheet Meltwater
361	Reduces Transient Warming and Climate Sensitivity Through the Sea-Surface

362	Temperature Pattern Effect. Geophysical Research Letters, 49(24), e2022GL101249.
363	https://doi.org/10.1029/2022GL101249
364	Dong, Y., Polvani, L. M., Hwang, YT., & England, M. R. (2025). Stratospheric ozone
365	depletion has contributed to the recent tropical La Niña-like cooling pattern. Npj Climate
366	and Atmospheric Science, 8(1), 150. https://doi.org/10.1038/s41612-025-01020-0
367	Dunne, J. P., Horowitz, L. W., Adcroft, A. J., Ginoux, P., Held, I. M., John, J. G., Krasting, J. P.
368	Malyshev, S., Naik, V., Paulot, F., Shevliakova, E., Stock, C. A., Zadeh, N., Balaji, V.,
369	Blanton, C., Dunne, K. A., Dupuis, C., Durachta, J., Dussin, R., Zhao, M. (2020). The
370	GFDL Earth System Model Version 4.1 (GFDL-ESM 4.1): Overall Coupled Model
371	Description and Simulation Characteristics. Journal of Advances in Modeling Earth
372	Systems, 12(11), e2019MS002015. https://doi.org/10.1029/2019MS002015
373	Eyring, V., Bony, S., Meehl, G. A., Senior, C. A., Stevens, B., Stouffer, R. J., & Taylor, K. E.
374	(2016). Overview of the Coupled Model Intercomparison Project Phase 6 (CMIP6)
375	experimental design and organization. Geoscientific Model Development, 9(5), 1937-
376	1958. https://doi.org/10.5194/gmd-9-1937-2016
377	Fan, T., Deser, C., & Schneider, D. P. (2014). Recent Antarctic sea ice trends in the context of
378	Southern Ocean surface climate variations since 1950. Geophysical Research Letters,
379	41(7), 2419–2426. https://doi.org/10.1002/2014GL059239
380	Fyke, J., Sergienko, O., Löfverström, M., Price, S., & Lenaerts, J. T. M. (2018). An Overview of
381	Interactions and Feedbacks Between Ice Sheets and the Earth System. Reviews of
382	Geophysics, 56(2), 361–408. https://doi.org/10.1029/2018RG000600

383	Golledge, N. R., Keller, E. D., Gomez, N., Naughten, K. A., Bernales, J., Trusel, L. D., &
384	Edwards, T. L. (2019). Global environmental consequences of twenty-first-century ice-
385	sheet melt. Nature, 566(7742), 65-72. https://doi.org/10.1038/s41586-019-0889-9
386	He, C., Clement, A. C., Kramer, S. M., Cane, M. A., Klavans, J. M., Fenske, T. M., & Murphy,
387	L. N. (2023). Tropical Atlantic multidecadal variability is dominated by external forcing.
388	Nature, 622(7983), 521-527. https://doi.org/10.1038/s41586-023-06489-4
389	Held, I. M., Guo, H., Adcroft, A., Dunne, J. P., Horowitz, L. W., Krasting, J., Shevliakova, E.,
390	Winton, M., Zhao, M., Bushuk, M., Wittenberg, A. T., Wyman, B., Xiang, B., Zhang, R.,
391	Anderson, W., Balaji, V., Donner, L., Dunne, K., Durachta, J., Zadeh, N. (2019).
392	Structure and Performance of GFDL's CM4.0 Climate Model. Journal of Advances in
393	Modeling Earth Systems, 11(11), 3691–3727. https://doi.org/10.1029/2019MS001829
394	Hwang, YT., Xie, SP., Deser, C., & Kang, S. M. (2017). Connecting tropical climate change
395	with Southern Ocean heat uptake: Tropical Climate Change and SO Heat Uptake.
396	Geophysical Research Letters, 44(18), 9449–9457.
397	https://doi.org/10.1002/2017GL074972
398	Kang, S. M. (2020). Extratropical Influence on the Tropical Rainfall Distribution. Current
399	Climate Change Reports, 6(1), 24–36. https://doi.org/10.1007/s40641-020-00154-y
400	Kang, S. M., Hawcroft, M., Xiang, B., Hwang, YT., Cazes, G., Codron, F., Crueger, T., Deser,
401	C., Hodnebrog, Ø., Kim, H., Kim, J., Kosaka, Y., Losada, T., Mechoso, C. R., Myhre, G.
402	Seland, Ø., Stevens, B., Watanabe, M., & Yu, S. (2019). ETIN-MIP Extratropical-
403	Tropical Interaction Model Intercomparison Project – Protocol and Initial Results.
404	Bulletin of the American Meteorological Society. https://doi.org/10.1175/BAMS-D-18-
405	0301.1

106	Kang, S. M., Yu, Y., Deser, C., Zhang, X., Kang, IS., Lee, SS., Rodgers, K. B., & Ceppi, P.
107	(2023). Global impacts of recent Southern Ocean cooling. Proceedings of the National
804	Academy of Sciences, 120(30), e2300881120. https://doi.org/10.1073/pnas.2300881120
109	Kaufman, Z., Wilson, E., Purich, A., Beadling, R., & Li, Y. (2025). The Impact of
110	Underestimated Southern Ocean Freshening on Simulated Historical Sea Surface
111	Temperature Trends. Geophysical Research Letters, 52(6), e2024GL112639.
112	https://doi.org/10.1029/2024GL112639
113	Kelley, M., Schmidt, G. A., Nazarenko, L. S., Bauer, S. E., Ruedy, R., Russell, G. L., Ackerman,
114	A. S., Aleinov, I., Bauer, M., Bleck, R., Canuto, V., Cesana, G., Cheng, Y., Clune, T. L.,
115	Cook, B. I., Cruz, C. A., Del Genio, A. D., Elsaesser, G. S., Faluvegi, G., Yao, MS.
116	(2020). GISS-E2.1: Configurations and Climatology. Journal of Advances in Modeling
117	Earth Systems, 12(8), e2019MS002025. https://doi.org/10.1029/2019MS002025
118	Kim, H., Kang, S. M., Kay, J. E., & Xie, SP. (2022). Subtropical clouds key to Southern Ocean
119	teleconnections to the tropical Pacific. Proceedings of the National Academy of Sciences,
120	119(34), e2200514119. https://doi.org/10.1073/pnas.2200514119
121	Klein, S. A., Hall, A., Norris, J. R., & Pincus, R. (2017). Low-Cloud Feedbacks from Cloud-
122	Controlling Factors: A Review. Surveys in Geophysics, 38(6), 1307–1329.
123	https://doi.org/10.1007/s10712-017-9433-3
124	Kuhlbrodt, T., Jones, C. G., Sellar, A., Storkey, D., Blockley, E., Stringer, M., Hill, R., Graham,
125	T., Ridley, J., Blaker, A., Calvert, D., Copsey, D., Ellis, R., Hewitt, H., Hyder, P., Ineson,
126	S., Mulcahy, J., Siahaan, A., & Walton, J. (2018). The Low-Resolution Version of
127	HadGEM3 GC3.1: Development and Evaluation for Global Climate. Journal of Advance.
128	in Modeling Earth Systems, 10(11), 2865–2888. https://doi.org/10.1029/2018MS001370

429	Liu, Z., & Alexander, M. (2007). Atmospheric bridge, oceanic tunnel, and global climatic
430	teleconnections. Reviews of Geophysics, 45(2). https://doi.org/10.1029/2005RG000172
431	Mantua, N. J., Hare, S. R., Zhang, Y., Wallace, J. M., & Francis, R. C. (1997). A Pacific
432	Interdecadal Climate Oscillation with Impacts on Salmon Production*. Bulletin of the
433	American Meteorological Society, 78(6), 1069–1080. https://doi.org/10.1175/1520-
434	0477(1997)078%253C1069:APICOW%253E2.0.CO;2
435	Morrison, A. K., England, M. H., & Hogg, A. M. (2015). Response of Southern Ocean
436	Convection and Abyssal Overturning to Surface Buoyancy Perturbations.
437	https://doi.org/10.1175/JCLI-D-14-00110.1
438	Purich, A., Cai, W., England, M. H., & Cowan, T. (2016). Evidence for link between modelled
439	trends in Antarctic sea ice and underestimated westerly wind changes. Nature
440	Communications, 7(1), 10409. https://doi.org/10.1038/ncomms10409
441	Purich, A., England, M. H., Cai, W., Chikamoto, Y., Timmermann, A., Fyfe, J. C., Frankcombe,
442	L., Meehl, G. A., & Arblaster, J. M. (2016). Tropical Pacific SST Drivers of Recent
443	Antarctic Sea Ice Trends. Journal of Climate, 29(24), 8931–8948.
444	https://doi.org/10.1175/JCLI-D-16-0440.1
445	Purich, A., England, M. H., Cai, W., Sullivan, A., & Durack, P. J. (2018). Impacts of Broad-
446	Scale Surface Freshening of the Southern Ocean in a Coupled Climate Model. Journal of
447	Climate, 31(7), 2613–2632. https://doi.org/10.1175/JCLI-D-17-0092.1
448	Roach, L. A., Mankoff, K. D., Romanou, A., Blanchard-Wrigglesworth, E., Haine, T. W. N., &
449	Schmidt, Gavin. A. (2023). Winds and Meltwater Together Lead to Southern Ocean
450	Surface Cooling and Sea Ice Expansion. Geophysical Research Letters, 50(24),
451	e2023GL105948. https://doi.org/10.1029/2023GL105948

Rugenstein, M., Zelinka, M., Karnauskas, K., Ceppi, P., & Andrews, T. (2023). Patterns of 452 Surface Warming Matter for Climate Sensitivity. Eos, 104. 453 https://doi.org/10.1029/2023EO230411 454 Rye, C. D., Marshall, J., Kelley, M., Russell, G., Nazarenko, L. S., Kostov, Y., Schmidt, G. A., 455 & Hansen, J. (2020). Antarctic Glacial Melt as a Driver of Recent Southern Ocean 456 Climate Trends. Geophysical Research Letters, 47(11), e2019GL086892. 457 https://doi.org/10.1029/2019GL086892 458 Sadai, S., Condron, A., DeConto, R., & Pollard, D. (2020). Future climate response to Antarctic 459 Ice Sheet melt caused by anthropogenic warming. Science Advances, 6(39), eaaz1169. 460 https://doi.org/10.1126/sciadv.aaz1169 461 Seo, J., Kang, S. M., & Frierson, D. M. W. (2014). Sensitivity of Intertropical Convergence Zone 462 Movement to the Latitudinal Position of Thermal Forcing. https://doi.org/10.1175/JCLI-463 D-13-00691.1 464 Stevens, B., Sherwood, S. C., Bony, S., & Webb, M. J. (2016). Prospects for narrowing bounds 465 on Earth's equilibrium climate sensitivity. Earth's Future, 4(11), 512–522. 466 https://doi.org/10.1002/2016EF000376 467 468 Swart, N. C., Cole, J. N. S., Kharin, V. V., Lazare, M., Scinocca, J. F., Gillett, N. P., Anstey, J., Arora, V., Christian, J. R., Hanna, S., Jiao, Y., Lee, W. G., Majaess, F., Saenko, O. A., 469 470 Seiler, C., Seinen, C., Shao, A., Sigmond, M., Solheim, L., ... Winter, B. (2019). The Canadian Earth System Model version 5 (CanESM5.0.3). Geoscientific Model 471 472 Development, 12(11), 4823–4873. https://doi.org/10.5194/gmd-12-4823-2019 Swart, N. C., Martin, T., Beadling, R., Chen, J.-J., Danek, C., England, M. H., Farneti, R., 473 Griffies, S. M., Hattermann, T., Hauck, J., Haumann, F. A., Jüling, A., Li, Q., Marshall, 474

475	J., Muilwijk, M., Pauling, A. G., Purich, A., Smith, I. J., & Thomas, M. (2023). The
476	Southern Ocean Freshwater Input from Antarctica (SOFIA) Initiative: Scientific
477	objectives and experimental design. Geoscientific Model Development, 16(24), 7289-
478	7309. https://doi.org/10.5194/gmd-16-7289-2023
479	Watanabe, M., Kang, S. M., Collins, M., Hwang, YT., McGregor, S., & Stuecker, M. F. (2024)
480	Possible shift in controls of the tropical Pacific surface warming pattern. Nature,
481	630(8016), 315–324. https://doi.org/10.1038/s41586-024-07452-7
482	Wills, R. C. J., Dong, Y., Proistosecu, C., Armour, K. C., & Battisti, D. S. (2022). Systematic
483	Climate Model Biases in the Large-Scale Patterns of Recent Sea-Surface Temperature
484	and Sea-Level Pressure Change. Geophysical Research Letters, 49(17), e2022GL100011
485	https://doi.org/10.1029/2022GL100011
486	Xie, SP., Deser, C., Vecchi, G. A., Ma, J., Teng, H., & Wittenberg, A. T. (2010). Global
487	Warming Pattern Formation: Sea Surface Temperature and Rainfall*. Journal of Climate
488	23(4), 966–986. https://doi.org/10.1175/2009JCLI3329.1
489	Zhang, X., & Deser, C. (2024). Tropical and Antarctic sea ice impacts of observed Southern
490	Ocean warming and cooling trends since 1949. Npj Climate and Atmospheric Science,
491	7(1), 1–9. https://doi.org/10.1038/s41612-024-00735-w
492	Zhang, X., Deser, C., & Sun, L. (2021). Is There a Tropical Response to Recent Observed
493	Southern Ocean Cooling? Geophysical Research Letters, 48(5), e2020GL091235.
494	https://doi.org/10.1029/2020GL091235
495	Ziehn, T., Chamberlain, M. A., Law, R. M., Lenton, A., Bodman, R. W., Dix, M., Stevens, L.,
496	Wang, YP., & Srbinovsky, J. (2020). The Australian Earth System Model: ACCESS-

ESM1.5. Journal of Southern Hemisphere Earth Systems Science, 70(1), 193–214.

https://doi.org/10.1071/ES19035